Psychological Medicine

cambridge.org/psm

Altered brain structural and functional connectivity in schizotypy

Yong-ming Wang[1,2,3,4], Xin-lu Cai[1,2,3,4], Rui-ting Zhang[1,4], Yi-jing Zhang[1,4], Han-yu Zhou[1,4], Yi Wang[1,4], Ya Wang[1,4], Jia Huang[1,4], Yan-yu Wang[1,5], Eric F. C. Cheung[6] and Raymond C. K. Chan[1,2,3,4]

[1]Neuropsychology and Applied Cognitive Neuroscience Laboratory, CAS Key Laboratory of Mental Health, Institute of Psychology, Beijing 100101, PR China; [2]Sino-Danish College, University of Chinese Academy of Sciences, Beijing 100190, PR China; [3]Sino-Danish Center for Education and Research, Beijing 100190, PR China; [4]Department of Psychology, University of Chinese Academy of Sciences, Beijing, PR China; [5]Department of Psychology, Weifang Medical University, Shandong Province, PR China and [6]Castle Peak Hospital, Hong Kong Special Administrative Region, PR China

Original Article

Cite this article: Wang Yong-ming *et al* (2022). Altered brain structural and functional connectivity in schizotypy. *Psychological Medicine* **52**, 834–843. https://doi.org/10.1017/S0033291720002445

Received: 12 November 2019
Revised: 15 June 2020
Accepted: 24 June 2020
First published online: 17 July 2020

Key words:
Connectivity decompensation hypothesis; dynamic functional connectivity; schizotypy; static functional connectivity; structural connectivity probability

Author for correspondence:
Raymond C. K. Chan,
E-mail: rckchan@psych.ac.cn

Abstract

Background. Schizotypy refers to schizophrenia-like traits below the clinical threshold in the general population. The pathological development of schizophrenia has been postulated to evolve from the initial coexistence of 'brain disconnection' and 'brain connectivity compensation' to 'brain connectivity decompensation'.

Methods. In this study, we examined the brain connectivity changes associated with schizotypy by combining brain white matter structural connectivity, static and dynamic functional connectivity analysis of diffusion tensor imaging data and resting-state functional magnetic resonance imaging data. A total of 87 participants with a high level of schizotypal traits and 122 control participants completed the experiment. Group differences in whole-brain white matter structural connectivity probability, static mean functional connectivity strength, dynamic functional connectivity variability and stability among 264 brain sub-regions of interests were investigated.

Results. We found that individuals with high schizotypy exhibited increased structural connectivity probability within the task control network and within the default mode network; increased variability and decreased stability of functional connectivity within the default mode network and between the auditory network and the subcortical network; and decreased static mean functional connectivity strength mainly associated with the sensorimotor network, the default mode network and the task control network.

Conclusions. These findings highlight the specific changes in brain connectivity associated with schizotypy and indicate that both decompensatory and compensatory changes in structural connectivity within the default mode network and the task control network in the context of whole-brain functional disconnection may be an important neurobiological correlate in individuals with high schizotypy.

Introduction

Schizotypy refers to subclinical schizophrenia-like traits found in the general population (Meehl, 1962; Sarig, Dar, & Liberman, 2012). Its clinical manifestations include cognitive-perceptual (positive), interpersonal (negative), and cognitive disorganized features (Polner et al., 2019; Raine et al., 1994), which are qualitatively similar to schizophrenia symptoms and correlate with schizophrenia liability (Grant, Green, & Mason, 2018). Schizotypy may represent an 'endophenotype' on the path to schizophrenia (Grant, 2015), and can be quantitatively assessed using the Schizotypal Personality Questionnaire (SPQ; Raine, 1991). Epidemiological studies have shown that the proportion of individuals with a high level of schizotypal traits in the general population is about 10% (Ettinger, Meyhöfer, Steffens, Wagner, & Koutsouleris, 2014; Lenzenweger, 2011). Studying schizotypy could help in understanding schizophrenia-related psychopathology (Kwapil & Barrantes-Vidal, 2014) and putative schizophrenia endophenotypes (Lenzenweger, 2015).

Previous studies have suggested that the neurobiological basis of schizophrenia may be 'brain disconnection' or 'brain dysconnection' (Friston, Brown, Siemerkus, & Stephan, 2016; Friston & Frith, 1995; Stephan, Friston, & Frith, 2009; Wang et al., 2018b). Specifically, one study has found that fractional anisotropy values of the fronto-temporal white matter tracts correlated negatively with scores on the SPQ cognitive-perceptual subscale in the general population (Nelson et al., 2011). Resting-state functional magnetic resonance imaging (rs-fMRI) studies have found that individuals with a high level of schizotypal traits exhibited reduced functional connectivity between the precuneus and the parahippocampus, which was

© The Author(s), 2020. Published by Cambridge University Press

CAMBRIDGE UNIVERSITY PRESS

negatively correlated with SPQ total scores (Zhu et al., 2017). In the general population, SPQ cognitive-perceptual subscale scores correlated positively with functional connectivity between the ventral striatum and the frontal cortex, and negatively with the functional connectivity between the dorsal striatum and the posterior cingulate cortex (Wang, Ettinger, Meindl, & Chan, 2018a, 2018b). An independent component analysis study found that SPQ cognitive-perceptual subscale scores correlated positively with low-frequency oscillations of the visual network, while SPQ interpersonal subscale scores correlated negatively with low-frequency oscillations of the auditory network in the general population (Lagioia, Van De Ville, Debbané, Lazeyras, & Eliez, 2010). These findings suggest that the development of schizotypy may be related to changed brain network connectivity (Mohr & Claridge, 2015). Comprehensive investigation in individuals with a high level of schizotypal traits could enhance our understanding of the differences and similarities in structural and functional connectivity changes associated with schizotypy and could identify which of these changes are important in individuals with high schizotypy (Lenzenweger, 2006).

Previous studies on schizotypy have also paid little attention to the time dynamics of functional connectivity. Temporal coupling between brain sub-regions is time-variant rather than time-invariant (Nomi et al., 2017). Dynamic functional connectivity (DFC), also called 'chronnectome', could provide insight into the mutability of interacted functional connectivity networks. One previous study has found that schizophrenia patients exhibited dynamic changes in thalamic hyperconnectivity and sensory hypoconnectivity (Damaraju et al., 2014). Another study found that individuals with psychotic-like experiences exhibited altered brain dynamics associated with hyperconnectivity of the visual network and hypoconnectivity of the default mode network (Barber, Lindquist, DeRosse, & Karlsgodt, 2018). Overall, the stability of DFC in individuals with high level of schizotypal traits warrants further investigation.

In this study, we investigated the structural connectivity, static functional connectivity and DFC using diffusion tensor imaging (DTI), and resting-state functional magnetic resonance imaging (rs-fMRI) technology. We estimated structural connectivity by probabilistic tractography and DFC by a new and reliable Dynamic Conditional Correlation (DCC) method (Lindquist, Xu, Nebel, & Caffo, 2014), which is more reliable than slide-window and non-parametric estimation methods with a quantitative description of time-varying characteristics (Choe et al., 2017). The representative whole-brain template we used in this study was identified by Power et al. (2011), which included 264 regions of interest (ROI) belonging to diverse brain networks. The structural connectivity probability, the static mean functional connectivity strength and DFC indices including the DFC variability and the DFC stability between these ROIs were calculated.

Based on previous findings of both deficits and compensatory brain connectivity changes between brain regions or networks associated with the development of schizophrenia spectrum disorder (Abram et al., 2017; Andreasen, Paradiso, & O'leary, 1998; Chan et al., 2011; Cho et al., 2015; Pettersson-Yeo, Allen, Benetti, McGuire, & Mechelli, 2011), we propose a neurobiological developmental possibility of schizophrenia called the 'Connectivity Decompensation Hypothesis', which hypothesize that the pathological development of schizophrenia spectrum continuum is a gradual process from functional compensation to partial decompensation to complete decompensation. In this model, some neural circuits associated with emotion, sensory and perceptual inference may gradually become impaired in susceptible individuals due to a combination of genetic and/or undesirable internal and external environmental factors (Friston et al., 2016). These abnormalities could still be partially compensated initially and these individuals could maintain normal functioning by gradual structural proliferation, remyelination, adaptive functional adjustment or reorganization of brain sub-regions associated with cognitive regulation and self-monitoring (Mohr & Claridge, 2015). The majority of them would never develop the illness. However, if these predisposing factors are excessive and persistent, or if neural compensation mechanisms fail, psychotic-like features and cognitive function maladjustment could be further aggravated, leading to clinical illness onset. Individuals with a high level of schizotypal traits are in the early stage of this process, and investigation of them could offer the best opportunity for early intervention and prevention and avoid confounding factors such as antipsychotic medication exposure and psychiatric comorbidities (Barrantes-Vidal, Grant, & Kwapil, 2015).

Thus, the objectives of our study were (1) to investigate common and specific changes in functional and structural connectivity in individuals with a high level of schizotypal traits compared with controls; and (2) to verify the connectivity decompensation hypothesis in individuals with a high level of schizotypal traits. If functional and structural connectivity between ROIs were both increased in the high schizotypy group, it could be considered as a compensation effect in this pathway. If functional connectivity between ROIs were decreased while structural connectivity was increased, it could imply decompensation. Based on previous studies, we hypothesized that changes in structural and functional connectivity in individuals with a high level of schizotypal traits would exhibit both decompensatory and compensatory effects, which could indicate 'brain disconnection'.

Material and methods

Participants

We first collected 4000 online schizotypal personality questionnaire (SPQ) responses from various universities randomly in Beijing through advertisement in 2018. Every voluntary participant was a college student and was paid. The 90th percentile of the SPQ total score (41 points) among these participants was taken as the cut-off score, which was in accord with previous studies setting individuals scoring in the top 10% of SPQ scores in the general population as the high schizotypy group (Chan et al., 2011; Ettinger et al., 2014; Lenzenweger, 2011; Shan et al., 2020; Shi et al., 2017; Wang et al., 2014, 2020a, 2020b). Students with a score above 41 were assigned to the high schizotypy group, and those with a score below 41 were assigned as controls. Then individuals allocated to the high schizotypy group and a corresponding number of controls were contacted by text message to invite them to participate in the subsequent MRI experiment. Of the total, 90% of the participants responded to the online survey. Of which, 246 responders agreed to undertake the brain scan. Inclusion criteria for all participants included Han ethnicity and aged 18 years or above. Exclusion criteria for all participants included any diagnosis of physical or psychiatric disorders and substance dependence, any family history of psychiatric disorder and any contraindications for MRI scanning. In addition, any participant who did not complete all study procedures, whose imaging quality was poor, and who had head motions greater

https://doi.org/10.1017/S0033291720002445 Published online by Cambridge University Press

than 2 mm and/or 2° during scanning were excluded. With these criteria, 35 participants were excluded. The study was approved by the Ethics Committee of the Department of Psychology, the University of the Chinese Academy of Sciences. All participants gave written informed consent.

Questionnaire assessment

The SPQ is a 74-item self-assessment scale that assesses schizotypal traits (Raine, 1991). These items can be clustered into three factors, namely the cognition-perceptual, interpersonal and disorganization factors (Chen, Hsiao, & Lin, 1997). The Chinese version of the SPQ has been shown to possess good psychometric properties (Cronbach α coefficient = 0.91, test-retest reliability = 0.82; Chen et al., 1997; Wang et al., 2013). The intelligence quotient (IQ) of all participants was estimated with the short-form of the Chinese version of the Wechsler Adult Intelligence Scale – Revised (Gong, 1992). The participants were asked to fill in the SPQ again before MRI scanning so that their SPQ scores were determined on the same day as the IQ estimation.

MRI acquisition

After the participants had completed the questionnaire assessment, resting-state functional magnetic resonance (rs-fMRI), anatomical and diffusion tensor images (DTI) were acquired in sequence using a 3.0 T GE MR scanner at the Institute of Psychology, the Chinese Academy of Sciences, Beijing, China from 2018 to 2019. Rs-fMRI was obtained using a T2-weighted echo planar imaging (EPI) sequence. Three hundred volumes were acquired with 37 slices, a slice thickness of 3.5 mm, a slice spacing of 0.5 mm, repetition time (TR) of 2000 ms, echo time (TE) of 30 ms, a field of view (FOV) of 220 mm, flip angle of 90°, in-plane acquisition matrix size of 64 × 64, and voxel size of $3.4 \times 3.4 \times 4$ mm^3.

The anatomical images were obtained using a T1-weighted sagittal oriented magnetization prepared rapid gradient echo (MPRAGE) sequence with the following parameters: 176 slices, a slice thickness of 1 mm, TR of 6.90 ms, TE of 2.99 ms, FOV of 256 mm, flip angle of 8°, inversion time of 450 ms, matrix size of 256 × 256, and voxel size of $1 \times 1 \times 1$ mm^3.

DTI with 64 directions were acquired with a spin echo pulse sequence: 74 slices, thickness of 2 mm, TR of 8500 ms, TE of 81 ms, FOV of 256 mm, flip angle of 90°, *b*-value of 1000 s/mm^2, matrix size of 128 × 128, and voxel size of $2 \times 2 \times 2$ mm^3.

DTI data preprocessing

DTI data were preprocessed by the FSL (https://fsl.fmrib.ox.ac.uk/fsl; Smith et al., 2006) and PANDA 1.3.1 (http://www.nitrc.org/projects/panda; Cui, Zhong, Xu, He, & Gong, 2013). The processing was the same as our another schizophrenia DTI study (Wang et al., 2020a). The data weres first screened by an experienced radiologist to rule out incidental structural abnormalities. Two participants were excluded. The raw images were then cropped using the fslroi command of the FSL (for DWI, f(skull removal) of 0.25; for T1 imaging, f(skull removal) of 0.5; cropping gap is 3 mm). Correction of DWI eddy-current induced distortion and head motion during scanning was then carried out. DWI was registered to the *b*-value of 0 images with affine transformation (the average of these *b*-values was used as reference). Individual images in native space were normalized to the FMRIB58_FA template (https://fsl.fmrib.ox.ac.uk/fsl/fslwiki/FMRIB58_FA) in MNI space (Mori et al., 2008), and smoothed using a 6 mm Gaussian kernel. Then test bvecs utility was used to find the correct Invert and Swap parameter of the DWI orientation. BedpostX was used to build up distributions on diffusion parameters at each voxel and create all the files necessary for running the next probabilistic tractography procedure with the following parameters: fibres = 2, weight = 1, and Burn-in = 1000 (Behrens, Berg, Jbabdi, Rushworth, & Woolrich, 2007). Probabilistic tractography between 264 ROIs with 6 mm radius was performed with the following parameters: curvature threshold = 0.2, maximum number of steps = 1000, step length = 0.5 mm, number of samples = 50 000, and tracking type of path distribution (Cho et al., 2015). For each ROI, probabilistic tractography was performed by seeding from all voxels in a particular ROI. The white matter connection probability from ROI *i* to ROI *j* was defined by the number of water molecules passing through ROIs divided by the total number of fibres sampled from the ROIs (Behrens et al., 2007). A 264 ROIs × 264 ROIs probabilistic matrix was generated for every participant. Then a threshold value of 0.001 was applied to reduce false-positive connections between ROIs (Fang et al., 2012). Since the connection probability from region *i* to region *j* was not necessarily equivalent to the one from *j* to *i*, these two probabilities were averaged to acquire a symmetrical non-directional connectivity matrix for each participant, which resulted in 34 716 connection probability values.

Rs-fMRI data preprocessing

Rs-fMRI data were preprocessed by the Statistical Parametric Mapping Software (SPM12, https://www.fil.ion.ucl.ac.uk/spm/) and Data Processing & Analysis for Brain Imaging (DPABI4.0, http://www.rfmri.org/dpabi) and brainwavelet 1.1 (http://www.brainwavelet.org) Software in MATLAB R2016b (MathWorks Inc., https://www.mathworks.com; Patel et al., 2014; Yan & Zang, 2010). The first 10 volumes were discarded. Then slice timing, realignment and wavelet despiking were performed using DPABI and brainwavelet, respectively. Subsequently, nuisance covariates, including Friston 24 head motion parameters, white matter signal and cerebrospinal fluid signal were regressed out (Friston, Williams, Howard, Frackowiak, & Turner, 1996). Structural images were manually co-registered and realigned with the anterior commissure-posterior commissure line, and co-registered to the mean functional image, and segmented as grey matter, white matter and cerebrospinal fluid using DARTEL in SPM. Then each functional image was normalized to standard Montreal Neurological Institute space in $3 \times 3 \times 3$ mm^3 voxels and the images were then band-pass filtered (0.01–0.1 Hz). Spatial smoothing was performed with a 6 mm full-width at half-maximum kernel. The mean frame-wise displacement (FD) was included as a covariate in the subsequent analysis (Power, Barnes, Snyder, Schlaggar, & Petersen, 2012; Yan et al., 2013). The time series of 264 ROIs with 6 mm radius of each participant were then extracted. The resting-state fMRI networks were constructed using Pearson correlation in the DPABI 4.0, and dynamic brain networks were constructed using the dynamic conditional correlation (DCC) script in the dynamic connectivity toolbox of Martin Lindquist in MATLAB 2016b (Lindquist et al., 2014; https://github.com/canlab/ Lindquist_Dynamic_Correlation). A 264 ROIs × 264 ROIs static functional connectivity matrix and 264 ROIs × 264 ROIs × 290 time series DFC matrix of every

https://doi.org/10.1017/S0033291720002445 Published online by Cambridge University Press

participant were generated. The mean functional connectivity strength, the DFC standard deviation and the DFC stability of every connection between two ROIs were calculated, which resulted in 34 716 values. DFC standard deviation (variability) indicates the overall fluctuation level of DFC over time. DFC stability describes the continuousness of the temporal changes in DFC between adjacent time series (Liu, Liao, Xia, & He, 2018). The formula for DFC stability is:

$$\text{DFC stability}\,(i,j) = 1 - \frac{1}{(T-1)}\sum_{1}^{T-1}\left(\frac{|r_{(i,j)(t+1)} - r_{(i,j)t}|}{2}\right)$$

where $r_{(i,j)t}$ is the strength of functional connectivity between node i and node j at time t; T is the total number of time series: 290.

Data analysis

ANCOVA analysis of the mean functional connectivity strength, the DFC variability, the DFC stability, the white matter connectivity probability between the two groups was performed while regressing out the gender, age, IQ (FD values were also entered as a covariate in the functional connectivity analysis) based on a false discovery rate (FDR) of 0.05 using the network-based statistic software and Matlab 2016b (Verhoeven, Simonsen, & McIntyre, 2005; Zalesky, Fornito, & Bullmore, 2010). The resultant images were visualized with BrainNet Viewer (https://www.nitrc.org/projects/bnv; Xia, Wang, & He, 2013). Finally, Pearson correlation analysis were performed between connection probability and functional connectivity values with significant group differences and SPQ scores within the high schizotypy group while regressing out the gender, age, IQ (and FD in functional connectivity analysis) with a significance level set at FDR 0.05 correction using fdr_bh function in matlab 2016b (Benjamini & Hochberg, 1995).

Results

After screening and quality control, 87 individuals with high schizotypy and 122 controls were included in the final analysis. The mean age, IQ and FD of all participants was 21.44 years (S.D. = 2.18, range = 18–28 years), 124.89 (S.D. = 9.08, range = 90–145), 0.05 (S.D. = 0.02, range = 0.02–0.20) respectively. There were no significant differences between the two groups in gender, age, IQ and mean FD (38 men and 49 women, age = 21.17 ± 2.22, IQ = 125.15 ± 9.14, mean FD = 0.05 ± 0.03 in the high scizotypy group; 38 men and 84 women, age = 21.62 ± 2.15, IQ = 124.72 ± 9.04, mean FD = 0.05 ± 0.02 in the control group). The two groups differed significantly in SPQ scores (48.60 ± 5.53 in the high schizotypy group; 23.43 ± 10.62 in controls; $t = 20.22$, $p < 0.001$).

Compared with controls, the high schizotypy group exhibited increased white matter connectivity probability between the right insula (the cingulo-opercular task control network, COTCN) and the right middle frontal gyrus (the fronto-parietal task control network, FPTCN); between the left precuneus (the default mode network; DMN) and the left angular gyrus (the DMN); and increased DFC variability and decreased stability between the right precuneus (the DMN) and the left middle temporal gyrus (the DMN); as well as decreased stability between the right superior temporal gyrus (the auditory network) and the right putamen (the subcortical network), and between the left precuneus (the DMN) and the left middle occipital gyrus (the DMN).

In addition, 18 mean functional connectivity strength values exhibited significant between-group differences. Sixteen of them were decreased in the high schizotypy group compared with controls, which mainly involved the sensorimotor network, the auditory network, the visual network, the DMN and the task control network. Increased strength values were found between the left superior frontal gyrus (the FPTCN) and the right rolandic operculum area (the auditory network), and between the right superior frontal gyrus (the DMN) and the right medial superior frontal gyrus (medsFG, the DMN; see Table 1 and Fig. 1).

Correlation analysis in the high schizotypy group found that scores on the SPQ cognition-perceptual subscale were negatively correlated with the mean functional connectivity strength between the left middle occipital gyrus (the visual network) and the left inferior parietal lobule (the FPTCN; $r = -0.32$, $p = 0.003$).

Discussion

In this study, we investigated changes in both whole-brain structural and functional connectivity in individuals with a high level of schizotypal traits. We found increased DFC variability, decreased DFC stability, and static functional connectivity strength within sub-regions of the posterior DMN and within the task control network, and decreased static functional connectivity strength between the auditory network and the task control network in the high schizotypy group. At the same time, structural connectivity between them was significantly increased in the high schizotypy group. These results support our connectivity decompensation hypothesis in individuals with high schizotypy. However, we also found increased static functional connectivity strength within the sub-regions of the anterior DMN, and between the FPTCN and the auditory network, and increased structural connectivity between the FPTCN and the auditory network in the high schizotypy group, which may indicate compensatory effects. At the same time, we found both decreased static functional connectivity and structural connectivity between the superior temporal gyrus (the auditory network) and the angular gyrus (the FPTCN). It may represent impaired neural pathways. Finally, we did not find any pathway with both increased functional connectivity and decreased structural connectivity. Our findings could extend our understanding of the temporal dynamic coupling between brain sub-regions and may provide insight into the separated large-scale brain structural and functional connectivity patterns in the high schizotypy group (Loas, Monestes, Ingelaere, Noisette, & Herbener, 2009). Moreover, our results support our hypothesis of the coexistence of 'brain connectivity decompensation' and 'brain connectivity compensation' in individuals with a high level of schizotypal traits.

Previous meta-analytic studies have reported that schizophrenia patients mainly exhibit a reduction in structural connectivity, especially at the frontal lobe and the temporal lobe (Ellison-Wright & Bullmore, 2009; Pettersson-Yeo et al., 2011). In contrast, we found that individuals with high schizotypy exhibited increased white matter connectivity probability between the right insula (the COTCN) and the right middle frontal gyrus (mFG, the FPTCN), and between the left precuneus (the DMN) and the left angular gyrus (the DMN) compared with controls. The angular gyrus and the insula integrate and connect numerous surrounding regions (Seghier, 2013; Uddin, Nomi, Hebert-Seropian, Ghaziri, & Boucher, 2017) and increased structural

https://doi.org/10.1017/S0033291720002445 Published online by Cambridge University Press

https://doi.org/10.1017/S0033291720002445 Published online by Cambridge University Press

Table 1. Significant white and dynamic functional connectivity differences between the high schizotypal groups and controls

ROI	SCP in high schizotypy	SCP in controls	*t/p*	DFC S.D. in high schizotypy	DFC S.D. in controls	*t/p*	DFC sta in high schizotypy	DFC sta in controls	*t/p*	SFC values in high schizotypy	SFC values in controls	*t/p*
Precentral.R(SMN,29 −17 71) -angular.R (FPTCN, 37 −65 40)	2.58E-04 (2.40E-03)	4.19E-04 (2.35E-03)	*NaN*	7.12E-02 (6.77E-03)	7.14E-02 (6.85E-03)	*NaN*	9.73E-01 (2.84E-03)	9.73E-01 (4.83E-03)	*NaN*	−1.43E-01 (1.47E-01)	−7.14E-02 (1.59E-01)	*−12.05***
Precentral.R(SMN,20 −29 60) -iPL.L(FPTCN, −42 −55 45)	*0*	*0*	*NaN*	7.06E-02 (6.44E-03)	7.11E-02 (7.18E-03)	*NaN*	9.73E-01 (2.63E-03)	9.74E-01 (4.96E-03)	*NaN*	−1.17 E-01 (1.67E-01)	−3.54E-02 (1.91E-01)	*−13.99***
Precentral.R(SMN,20 −29 60) -mFG.L(DMN, −35 20 51)	*0*	*0*	*NaN*	7.02E-02 (6.45E-03)	7.14E-02 (7.31E-03)	*NaN*	9.73E-01 (2.58E-03)	9.73E-01 (4.88E-03)	*NaN*	−1.50E-01 (1.57E-01)	−6.33E-02 (1.67E-01)	*−16.95***
Precentral.L(SMN,−38 −15 69) –putamen.R (SCN, 23 10 1)	*0*	*0*	*NaN*	7.21E-02 (6.71E-03)	7.17E-02 (6.85E-03)	*NaN*	9.71E-01 (2.75E-03)	9.72E-01 (5.10E-03)	*NaN*	−8.78E-03 (1.22E-01)	5.35E-02 (1.28E-01)	*−12.88***
SMG.R(COTCN,54 −28 34) -mFG.R(SN,26 50 27)	*0*	*0*	*NaN*	6.99E-02 (7.21E-03)	7.01E-02 (8.94E-03)	*NaN*	9.74E-01 (2.99E-03)	9.74E-01 (4.99E-03)	*NaN*	−7.04E-02 (2.47E-01)	6.49E-02 (2.43E-01)	*−17.94**,*
Insula.R(COTCN,36 10 1) -mFG.R(FPTCN, 32 14 56)	*4.36E-03* (*1.36E-02*)	*3.43E-04* (*2.18E-03*)	*9.97***	7.04E-02 (6.85E-03)	7.08E-02 (7.29E-03)	*NaN*	9.73E-01 (2.91E-03)	9.74E-01 (4.91E-03)	*NaN*	−9.71E-02 (2.16E-01)	−1.00E-01 (1.99E-01)	*NaN*
sTG.R(AN,58 −16 7) -angular.R(FPTCN,37 −65 40)	1.19E-04 (1.11E-03)	1.12E-03 (4.32E-03)	*−4.70** p = 0.03*	7.10E-02 (6.72E-03)	7.20E-02 (6.36E-03)	*NaN*	9.73E-01 (2.72E-03)	9.73E-01 (4.91E-03)	*NaN*	−1.21E-01 (1.66E-01)	−2.50E-02 (1.62E-01)	*−21.32***
sTG.R(AN,58 −16 7) -putamen.R(SCN,31 −14 2)	1.38E-02 (1.93E-02)	1.37E-02 (2.13E-02)	*NaN*	6.58E-02 (8.69E-03)	6.27E-02 (9.80E-03)	*7.43** p = 0.007*	9.74E-01 (3.74E-03)	9.76E-01 (5.28E-03)	*−10.34***	3.56E-01 (1.97E-01)	4.30E-01 (2.20E-01)	***−9.04**** *p = 0.003*
ROA.R(AN,43 −23 20) -sFG.L(FPTCN,-23 11 64)	0	0	*NaN*	7.17E-02 (6.31E-03)	7.10E-02 (7.78E-03)	*NaN*	9.72E-01 (2.59E-03)	9.73E-01 (4.95E-03)	*NaN*	−2.54E-02 (1.51E-01)	−1.05E-01 (1.53E-01)	*14.94***
Heschl.L(AN,−30 −27 12) -iPL.L(FPTCN,−53 −49 43)	2.48E-02 (4.08E-02)	1.46E-02 (2.44E-02)	*4.87** p = 0.03*	7.20E-02 (6.74E-03)	7.22E-02 (6.72E-03)	*NaN*	9.72E-01 (2.84E-03)	9.73E-01 (5.10E-03)	*NaN*	−7.80E-02 (1.37E-01)	−7.33E-03 (1.43E-01)	*−13.42***
Heschl.L (AN,−30 −27 12) -iPL.L(FPTCN,−42 −55 45)	6.45E-03 (1.76E-02)	5.76E-03 (1.59E-02)	*NaN*	7.11E-02 (6.30E-03)	7.26E-02 (6.36E-03)	*NaN*	9.72E-01 (2.73E-03)	9.73E-01 (5.06E-03)	*NaN*	−9.85E-02 (1.53E-01)	−1.26E-02 (1.54E-01)	*−17.73***
Precuneus.L(DMN,−13 −40 1) -angular.L (DMN,−39 −75 44)	4.65E-03 (1.06E-02)	1.39E-03 (5.18E-03)	*9.31***	7.10E-02 (7.16E-03)	7.03E-02 (7.68E-03)	*NaN*	9.73E-01 (3.10E-03)	9.73E-01 (5.09E-03)	*NaN*	1.37E-01 (1.68E-01)	1.69E-01 (1.64E-01)	*NaN*
mTG.L(DMN,−46 −61 21) -precuneus.R (DMN,11 −54 17)	0	0	*NaN*	6.41E-02 (8.18E-03)	5.95E-02 (1.01E-02)	*12.67***	9.76E-01 (3.28E-03)	9.78E-01 (5.22E-03)	*−12.76***	4.22E-01 (1.77E-01)	5.39E-01 (2.17E-01)	*−17.43***
sFG.R(DMN,13 55 38) -medsFG.R(DMN,6 64 22)	6.40E-02 (8.30E-02)	7.42E-02 (7.91E-02)	*NaN*	5.72E-02 (1.32E-02)	6.17E-02 (1.10E-02)	*−8.55** p = 0.004*	9.79E-01 (5.26E-03)	9.78E-01 (5.46E-03)	*NaN*	5.72E-01 (3.24E-01)	4.41E-01 (2.77E-01)	*11.73***

https://doi.org/10.1017/S0033291720002445 Published online by Cambridge University Press

aCC.R(DMN,12 36 20) -mOG.L(VN,−26 −90 3)	0	0	*NaN*	7.19E-02 (6.79E-03)	7.07E-02 (8.10E-03)	*NaN*	9.73E-01 (2.89E-03)	9.74E-01 (4.88E-03)	*NaN*	5.51E-02 (1.44E-01)	1.23E-01 (1.53E-01)	*−12.14***
ioFG.L(DMN,−46 31 −13) -itFG.R(VAN,53 33 1)	0	0	*NaN*	6.36E-02 (9.67E-03)	5.89E-02 (1.16E-02)	*10.56* p = 0.001*	9.76E-01 (4.02E-03)	9.78E-01 (5.52E-03)	*−12.20* p = 0.001*	4.29E-01 (2.10E-01)	5.53E-01 (2.48E-01)	*−14.83***
mOG.L(VN,−40 −88 −6) -iPL.L(FPTCN,−28 −58 48)	0	0	*NaN*	7.02E-02 (8.72E-03)	6.80E-02 (8.45E-03)	*NaN*	9.74E-01 (3.50E-03)	9.75E-01 (4.96E-03)	*−6.18* p = 0.01*	1.15E-01 (2.35E-01)	2.50E-01 (2.32E-01)	*−17.77***
iOG.L(VN,−33 −79 −13) -iPL.L(FPTCN, −28 −58 48)	0	0	*NaN*	6.99E-02 (8.55E-03)	6.72E-02 (8.86E-03)	*6.09* p = 0.01*	9.74E-01 (3.26E-03)	9.75E-01 (5.14E-03)	*−7.22* p = 0.008*	1.58E-01 (2.48E-01)	2.99E-01 (2.39E-01)	*−17.54***
Precentral.R (FPTCN,47 10 33) -iPL.R(FPTCN,49 −42 45)	2.78E-03 (1.02E-02)	1.12E-03 (5.15E-03)	*NaN*	6.81E-02 (1.02E-02)	6.52E-02 (1.16E-02)	*NaN*	9.75E-01 (3.62E-03)	9.76E-01 (5.70E-03)	*−3.80* p = 0.05*	1.86E-01 (2.98E-01)	3.30E-01 (2.91E-01)	*−12.16***
Insula.L(SN,−35 20 0) -iTG.R(UN,46 −47 −17)	0	0	*NaN*	7.12E-02 (7.22E-03)	7.08E-02 (8.88E-03)	*NaN*	9.72E-01 (2.97E-03)	9.73E-01 (5.07E-03)	*NaN*	7.57E-02 (1.76E-01)	1.55E-01 (1.56E-01)	*−13.42***
mOG.L(DMN,−41 −75 26) – precuneus.L (DMN,−11 −56 16)	1.92E-04 (1.79E-03)	9.23E-05 (1.02E-03)	*NaN*	6.13E-02 (9.84E-03)	5.65E-02 (1.27E-02)	*8.95* p = 0.003*	9.77E-01 (3.72E-03)	9.79E-01 (5.78E-03)	*−11.62***	4.74E-01 (2.32E-01)	6.00E-01 (2.74E-01)	*−11.78***

ROI, region of interest; SCP, structural connection probability; DFC, dynamic functional connectivity; SFC, static functional connectivity; S.D., standard deviation; sta, stability; NaN, not a number or un-significant; DMN, default mode network; SN, salience network; VAN, ventral attention network; FPTCN, fronto-parietal task control network; COTCN, cingulo-opercular taskcontrol network; SMN, sensorimotor network; VN, visual network; AN, auditory network; SCN, subcortical network; UN, uncertain area; medsFG, medial superior frontal gyrus; ioFG, inferior frontal gyrus, orbital part; itFG, inferior frontal gyrus, triangular part; sFG, superior frontal gyrus; mFG, middle frontal gyrus; aCC, anterior cingulate cortex; iPL, inferior parietal lobule; mOG, middle occipital gyrus; iOG, inferior occipital gyrus; sTG, superior temporal gyrus; mTG, middle temporal gyrus; iTG, inferior temporal gyrus; SMG, supramarginal gyrus; ROA, rolandic operculum area; L, left; R, right; regions are presented as name (network, peak MNI coordinates); values are presented as means (standard deviation).

**FDR 0.05 corrected; *$p < 0.05$, uncorrected.

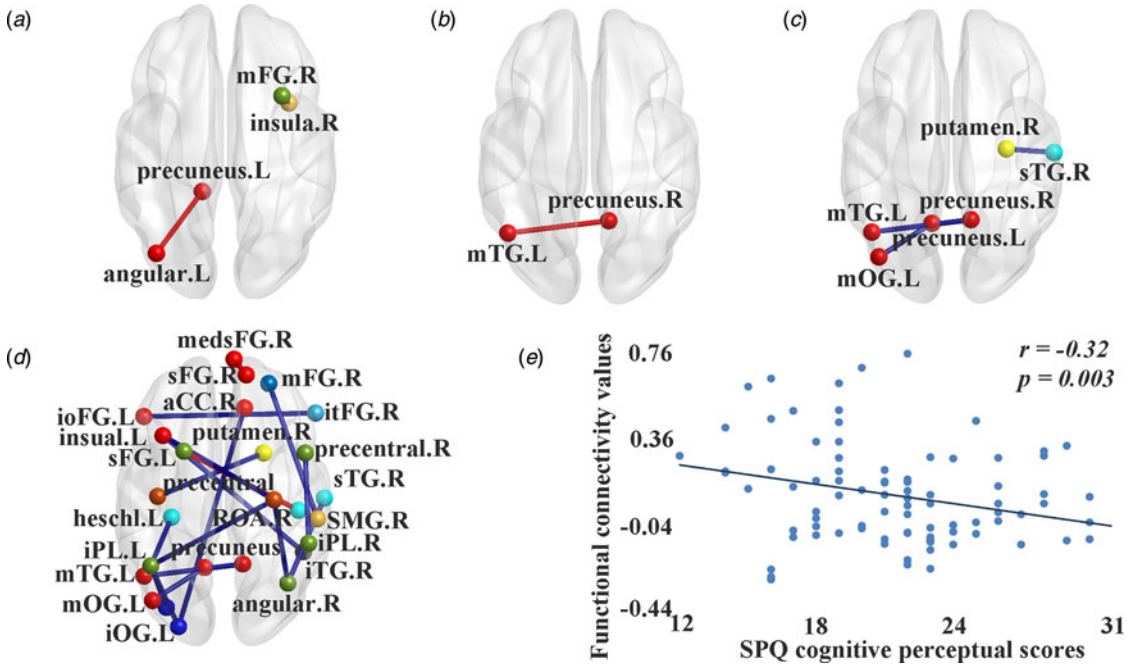


Fig. 1. Significant differences of white connectivity probability and functional connectivity values between individuals with high schizotypy and controls. (*a*) Significant differences in white matter connectivity probability. (*b*) Significant differences in dynamic functional connectivity variability. (*c*) Significant differences in dynamic functional connectivity stability. (*d*) Significant differences in static mean functional connectivity strength. (*e*) The negative correlation between SPQ cognitive-perceptual scores and static mean functional connectivity strength between the left middle occipital gyrus and the left inferior parietal lobule. In (*a–d*), red line, significant increased values in individuals with high schizotypy; blue line, significant decreased values in individuals with high schizotypy; red spot: sub-regions of the default mode network; light blue spot: sub-regions of the salience network; crimson spot: sub-regions of the sensorimotor network; blue spot: sub-regions of the visual network; green spot: sub-regions of the auditory network; cyan spot: sub-regions of the ventral attention network; lawngreen spot: sub-regions of the frontal-parietal task control network; orange spot: sub-regions of the cingulo-opercular task control network; yellow spot: sub-regions of the subcortical network; black spot: sub-regions of the uncertain area. SPQ, schizotypal personality questionnaire; medsFG, medial superior frontal gyrus; ioFG, inferior frontal gyrus, orbital part; itFG, inferior frontal gyrus, triangular part; sFG, superior frontal gyrus; mFG, middle frontal gyrus; aCC, anterior cingulate cortex; iPL, inferior parietal lobule; mOG, middle occipital gyrus; iOG, inferior occipital gyrus; sTG, superior temporal gyrus; mTG, middle temporal gyrus; iTG, inferior temporal gyrus; SMG, supramarginal gyrus; ROA, rolandic operculum area; L, left; R, right.

connectivity between these regions may represent a compensatory mechanism associated with synaptic plasticity and axonal proliferation, which mitigate dysfunctional executive control and self-sensory integration (Cai, Ryali, Chen, Li, & Menon, 2014; Nelson et al., 2011; Stephan et al., 2009; Zhu et al., 2017). Whether these compensatory changes in white matter pathways are effective or not could be speculated from their functional connectivity changes.

However, we also found that increased DFC variability decreased DFC stability, and static functional connectivity strength within sub-regions of the posterior DMN and within the task control network, and a negative correlation between SPQ cognition-perceptual subscale scores and the mean functional connectivity strength between the sub-regions of the visual network and the task control network in the high schizotypy group. These dysfunctions may be associated with unstable brain activity, disordered self-referential thought, and impaired consciousness (Crone et al., 2015; Hare et al., 2018), and may be the important neuro-functional basis of abnormal perception and suspiciousness in individuals with a high level of schizotypal traits (Wong & Raine, 2018). Together with the results of increased structural connectivity between them in the high schizotypy group, this may indicate discordant brain connectivity and ineffective neurological compensation between these regions in individuals with a high level of schizotypal traits, and support the presence of connectivity decompensation within the posterior DMN, and between the auditory network, the visual network and the task control network during the development of schizophrenia spectrum disorders.

Furthermore, the high schizotypy group also exhibited decreased DFC stability and static functional connectivity strength between sub-regions of the auditory network, the sensorimotor network and the putamen; as well as decreased static functional connectivity strength mainly between the sensorimotor network, the auditory network, the visual network, the DMN and the task control network compared with controls. The former may reflect that ineffective dopaminergic transmission for processing afferent sensory signals have already emerged in individuals with high schizotypy (Pawlak & Kerr, 2008). The latter may indicate dysfunctional segregation between auditory, visual, perceptual processing, and cognitive control ability (Carter et al., 2010; Rolland et al., 2015), deficits in self-awareness and external environmental information integration and perception-behaviour integration (Friston & Frith, 1995; Moore & Pope, 2014). These changes may be the key features associated with early psychosis proneness including cognitive disturbances (Kraguljac et al., 2016; Wang et al., 2018b; Woodward, Rogers, & Heckers, 2011), and the tendency to favour prior subjective knowledge rather than incoming sensory information (Friston et al., 2016; Rolland et al., 2015). Furthermore, most of these sub-regions with decreased functional connectivity features did not exhibit any changes in structural connectivity, suggesting that these

https://doi.org/10.1017/S0033291720002445 Published online by Cambridge University Press

dysfunctions may be caused by grey matter neuronal dendritic changes or mediated by other connectivity (Timmler & Simons, 2019).

In addition, we found increased static functional connectivity strength within the sub-regions of the anterior DMN, mainly between the superior frontal gyrus and the medsFG, and between sub-regions of the FPTCN and the auditory network, and increased structural connectivity between the FPTCN and the auditory network in the high schizotypy group. The increased connectivity between these sub-regions may indicate their self-adaptive efforts of advanced cognitive regulation for relieving sensorimotor and social-emotional dysfunction (Mohr & Claridge, 2015; Yin et al., 2011). This may be an important neurobiological compensatory mechanism for maintaining normal social behaviour in individuals with high schizotypy. The neurochemical basis of these changes may be due to the increase in functionally overlapping neural transmitters such as dopamine, glutamine, acetylcholine, and 5-hydroxytryptamine together with synaptic plasticity and axonal proliferation (Friston et al., 2016; Lau & Zukin, 2007; Miuller & Schwarz, 2007; Wolf, 2003; Wolf, Mangiavacchi, & Sun, 2003). We also found both decreased static functional connectivity and structural connectivity between the superior temporal gyrus (the auditory network) and the angular gyrus (the FPTCN) in the high schizotypy group. It may indicate defective axonal function associated with abnormal auditory sensory monitoring and self-referential processing (Cui et al., 2017; Friston et al., 2016).

Taken together, these structural and functional connectivity results may imply that enhanced connectivity within the DMN and within the task control network could not completely compensate for sensory-perceptual dysfunctional changes in individuals with a high level of schizotypal traits (Lindner, Thier, Kircher, Haarmeier, & Leube, 2005). The aberrant synaptic integration caused by hypofunction of the n-methyl-d-aspartate receptors (NMDAR) rather than axonal pathology may be the key neurochemical basis of the majority of decreased functional connectivity in individuals with high schizotypy (Tseng & O'Donnell, 2004; Wei et al., 2006), and these changes may correlate with schizophrenia genetic risk variants including DISC1, PPP1R1B, PRODH, and ZNF804A (Mothersill, Kelly, Rose, & Donohoe, 2012). Meanwhile, white matter structural alterations found in schizophrenia patients may be the pathophysiological consequence of deteriorating schizophrenia symptoms rather than the cause of the disorder (Friston et al., 2016).

This study has several limitations. First, we ascertained the absence of a psychiatric diagnosis, medication exposure, and history of psychiatric disorders of the participants only by self-report. The structured clinical interview should be adopted for higher validity in future studies. Secondly, it is difficult to clearly distinguish between compensatory and abnormal brain functional changes, and some other indirect pathways or dendritic connections between brain regions could also take effect (Timmler & Simons, 2019). Thus, our connectivity decompensation hypothesis requires further verification. Furthermore, the correlation between macroscopic connectivity and microscopic neurotransmitter and synaptic changes also requires further investigation. For example, inhibition of the dopamine D2 receptor could enhance NMDAR-dependent synaptic plasticity (Laruelle, Frankle, Narendran, Kegeles, & Abi-Dargham, 2005), which may be crucial for schizophrenia pathophysiology (Abi-Saab, D'ouza, Moghaddam, & Krystal, 1998; Hahn et al., 2006). Finally, investigations on specific schizotypal dimensions or symptoms are also important and future studies could focus on specific brain features of positive schizotypy or negative schizotypy or unusual perception or anhedonia.

In conclusion, our results suggest that individuals with high schizotypy exhibited both compensatory and deficient connectivity mainly associated with the DMN, the task control network and the sensorimotor network. Our results indicate the underlying brain connectivity adaptive changes in individuals with high schizotypy and provide a possible neurobiological basis for the connectivity decompensation hypothesis in schizophrenia spectrum disorders.

Acknowledgements. This work was supported by the National Key Research and Development Programme (2016YFC0906402), the Beijing Municipal Science & Technology Commission Grant (Z161100000216138), the Beijing Training Project for the Leading Talents in S & T (Z151100000315020), the Strategic Priority Research Program (B) of the Chinese Academy of Science (XDB02030002), and the CAS Key Laboratory of Mental Health, Institute of Psychology.

Author contributions.
YM Wang collected, analyzed and interpreted the data, and wrote up the drafts of the manuscript. YM Wang, XL Cai, RT Zhang, YJ Zhang, HY Zhou, YY Wang, Y Wang, Y Wang, and J Huang collected the data, administered assessment and interpreted the findings. EFC Cheung interpreted the findings and commented on the drafts critically. RCK Chan generated the idea, designed the study, interpreted the findings, and commented on the drafts critically.

Conflict of interest. The authors report no conflict of interest.

References

Abi-Saab, W. M., D'Souza, D. C., Moghaddam, B., & Krystal, J. H. (1998). The NMDA antagonist model for schizophrenia: Promise and pitfalls. *Pharmacopsychiatry*, *31*, 104–109.

Abram, S. V., Wisner, K. M., Fox, J. M., Barch, D. M., Wang, L., Csernansky, J. G., … Smith, M. J. (2017). Fronto-temporal connectivity predicts cognitive empathy deficits and experiential negative symptoms in schizophrenia. *Human Brain Mapping*, *38*, 1111–1124.

Andreasen, N. C., Paradiso, S., & O'leary, D. S. (1998). "Cognitive dysmetria" as an integrative theory of schizophrenia: A dysfunction in cortical-subcortical-cerebellar circuitry? *Schizophrenia Bulletin*, *24*, 203–218.

Barber, A. D., Lindquist, M. A., DeRosse, P., & Karlsgodt, K. H. (2018). Dynamic functional connectivity states reflecting psychotic-like experiences. *Biological Psychiatry: Cognitive Neuroscience and Neuroimaging*, *3*, 443–453.

Barrantes-Vidal, N., Grant, P., & Kwapil, T. R. (2015). The role of schizotypy in the study of the etiology of schizophrenia spectrum disorders. *Schizophrenia Bulletin*, *41*, S408–S416.

Behrens, T. E., Berg, H. J., Jbabdi, S., Rushworth, M., & Woolrich, M. (2007). Probabilistic diffusion tractography with multiple fibre orientations: What can we gain? *Neuroimage*, *34*, 144–155.

Benjamini, Y., & Hochberg, Y. (1995). Controlling the false discovery rate: A practical and powerful approach to multiple testing. *Journal of the Royal statistical society: series B (Methodological)*, *57*, 289–300.

Cai, W., Ryali, S., Chen, T., Li, C. S. R., & Menon, V. (2014). Dissociable roles of right inferior frontal cortex and anterior insula in inhibitory control: Evidence from intrinsic and task-related functional parcellation, connectivity, and response profile analyses across multiple datasets. *The Journal of Neuroscience*, *34*, 14652–14667.

Carter, A. R., Astafiev, S. V., Lang, C. E., Connor, L. T., Rengachary, J., Strube, M. J., … Corbetta, M. (2010). Resting interhemispheric functional magnetic resonance imaging connectivity predicts performance after stroke. *Annals of Neurology*, *67*, 365–375.

Chan, R. C., Yan, C., Qing, Y. H., Wang, Y., Wang, Y. N., Ma, Z., … Yu, X. (2011). Subjective awareness of everyday dysexecutive behavior precedes 'objective' executive problems in schizotypy: A replication and extension study. *Psychiatry Research*, *185*, 340–346.

https://doi.org/10.1017/S0033291720002445 Published online by Cambridge University Press

Chen, W. J., Hsiao, C. K., & Lin, C. C. (1997). Schizotypy in community samples: The three-factor structure and correlation with sustained attention. *Journal of Abnormal Psychology*, *106*, 649–654.

Cho, K. I. K., Shenton, M. E., Kubicki, M., Jung, W. H., Lee, T. Y., Yun, J. Y., … Kwon, J. S. (2015). Altered thalamo-cortical white matter connectivity: Probabilistic tractography study in clinical-high risk for psychosis and first-episode psychosis. *Schizophrenia Bulletin*, *42*, 723–731.

Choe, A. S., Nebel, M. B., Barber, A. D., Cohen, J. R., Xu, Y., Pekar, J. J., … Lindquist, M. A. (2017). Comparing test-retest reliability of dynamic functional connectivity methods. *Neuroimage*, *158*, 155–175.

Crone, J. S., Schurz, M., Höller, Y., Bergmann, J., Monti, M., Schmid, E., … Kronbichler, M. (2015). Impaired consciousness is linked to changes in effective connectivity of the posterior cingulate cortex within the default mode network. *Neuroimage*, *110*, 101–109.

Cui, L. B., Liu, L., Guo, F., Chen, Y. C., Chen, G., Xi, M., … Wang, H. N. (2017). Disturbed brain activity in resting-state networks of patients with first-episode schizophrenia with auditory verbal hallucinations: A cross-sectional functional MR imaging study. *Radiology*, *283*, 810–819.

Cui, Z., Zhong, S., Xu, P., He, Y., & Gong, G. (2013). PANDA: A pipeline toolbox for analyzing brain diffusion images. *Frontiers in Human Neuroscience*, *7*, 42.

Damaraju, E., Allen, E. A., Belger, A., Ford, J. M., McEwen, S., Mathalon, D. H., … Calhoun, V. D. (2014). Dynamic functional connectivity analysis reveals transient states of dysconnectivity in schizophrenia. *NeuroImage: Clinical*, *5*, 298–308.

Ellison-Wright, I., & Bullmore, E. (2009). Meta-analysis of diffusion tensor imaging studies in schizophrenia. *Schizophrenia Research*, *108*, 3–10.

Ettinger, U., Meyhöfer, I., Steffens, M., Wagner, M., & Koutsouleris, N. (2014). Genetics, cognition, and neurobiology of schizotypal personality: A review of the overlap with schizophrenia. *Frontiers in Psychiatry*, *5*, 18.

Fang, P., Zeng, L. L., Shen, H., Wang, L., Li, B., Liu, L., & Hu, D. (2012). Increased cortical-limbic anatomical network connectivity in major depression revealed by diffusion tensor imaging. *PLoS ONE*, *7*, e45972.

Friston, K., Brown, H., Siemerkus, J., & Stephan, K. (2016). The dysconnection hypothesis. *Schizophrenia Research*, *176*, 83–94.

Friston, K. J., & Frith, C. D. (1995). Schizophrenia: A disconnection syndrome. *Clinical Neuroscience*, *3*, 89–97.

Friston, K. J., Williams, S., Howard, R., Frackowiak, R. S., & Turner, R. (1996). Movement-related effects in fMRI time-series. *Magnetic Resonance in Medicine*, *35*, 346–355.

Gong, Y. (1992). *Manual of Wechsler adult intelligence scale-Chinese version*. Changsha: Chinese Map.

Grant, P. (2015). Is schizotypy per se a suitable endophenotype of schizophrenia? Do not forget to distinguish positive from negative facets. *Frontiers in Psychiatry*, *6*, 143.

Grant, P., Green, M. J., & Mason, O. J. (2018). Models of schizotypy: The importance of conceptual clarity. *Schizophrenia Bulletin*, *44*, S556–S563.

Hahn, C. G., Wang, H. Y., Cho, D. S., Talbot, K., Gur, R. E., Berrettini, W. H., … Arnold, S. E. (2006). Altered neuregulin 1-erbB4 signaling contributes to NMDA receptor hypofunction in schizophrenia. *Nature Medicine*, *12*, 824–828.

Hare, S. M., Ford, J. M., Mathalon, D. H., Damaraju, E., Bustillo, J., Belger, A., … Turner, J. A. (2018). Salience-default mode functional network connectivity linked to positive and negative symptoms of schizophrenia. *Schizophrenia Bulletin*, *45*, 892–901.

Kraguljac, N. V., White, D. M., Hadley, N., Hadley, J. A., ver Hoef, L., Davis, E., & Lahti, A. C. (2016). Aberrant hippocampal connectivity in unmedicated patients with schizophrenia and effects of antipsychotic medication: A longitudinal resting state functional MRI study. *Schizophrenia Bulletin*, *42*, 1046–1055.

Kwapil, T. R., & Barrantes-Vidal, N. (2014). Schizotypy: Looking back and moving forward. *Schizophrenia Bulletin*, *41*, S366–S373.

Lagioia, A., Van De Ville, D., Debbané, M., Lazeyras, F., & Eliez, S. (2010). Adolescent resting state networks and their associations with schizotypal trait expression. *Frontiers in Systems Neuroscience*, *4*, 35.

Laruelle, M., Frankle, W. G., Narendran, R., Kegeles, L. S., & Abi-Dargham, A. (2005). Mechanism of action of antipsychotic drugs: From dopamine D(2) receptor antagonism to glutamate NMDA facilitation. *Clinical Therapeutics*, *27*, S16–S24.

Lau, C. G., & Zukin, R. S. (2007). NMDA Receptor trafficking in synaptic plasticity and neuropsychiatric disorders. *Nature Reviews Neuroscience*, *8*, 413–426.

Lenzenweger, M. F. (2006). Schizotypy: An organizing framework for schizophrenia research. *Current Directions in Psychological Science*, *15*, 162–166.

Lenzenweger, M. F. (2011). *Schizotypy and schizophrenia: The view from experimental psychopathology*. New York: Guilford Press.

Lenzenweger, M. F. (2015). Thinking clearly about schizotypy: Hewing to the schizophrenia liability core, considering interesting tangents, and avoiding conceptual quicksand. *Schizophrenia Bulletin*, *41*, S483–S491.

Lindner, A., Thier, P., Kircher, T. T., Haarmeier, T., & Leube, D. T. (2005). Disorders of agency in schizophrenia correlate with an inability to compensate for the sensory consequences of actions. *Current Biology*, *15*, 1119–1124.

Lindquist, M. A., Xu, Y., Nebel, M. B., & Caffo, B. S. (2014). Evaluating dynamic bivariate correlations in resting-state fMRI: A comparison study and a new approach. *Neuroimage*, *101*, 531–546.

Liu, J., Liao, X., Xia, M., & He, Y. (2018). Chronnectome fingerprinting: Identifying individuals and predicting higher cognitive functions using dynamic brain connectivity patterns. *Human Brain Mapping*, *39*, 902–915.

Loas, G., Monestes, J. L., Ingelaere, A., Noisette, C., & Herbener, E. S. (2009). Stability and relationships between trait or state anhedonia and schizophrenic symptoms in schizophrenia: A 13-year follow-up study. *Psychiatry Research*, *166*, 132–140.

Meehl, P. E. (1962). Schizotaxia, schizotypy, schizophrenia. *American Psychologist*, *17*, 827–838.

Miuller, N., & Schwarz, M. J. (2007). The immunological basis of glutamatergic disturbance in schizophrenia: Towards an integrated view. *Journal of Neural Transplantation & Plasticity*, *72*, 269–280.

Mohr, C., & Claridge, G. (2015). Schizotypy-do not worry, it is not all worrisome. *Schizophrenia Bulletin*, *41*, S436–S443.

Moore, J. W., & Pope, A. (2014). The intentionality bias and schizotypy. *The Quarterly Journal of Experimental Psychology*, *67*, 2218–2224.

Mori, S., Oishi, K., Jiang, H., Jiang, L., Li, X., Akhter, K., … Mazziotta, J. (2008). Stereotaxic white matter atlas based on diffusion tensor imaging in an ICBM template. *Neuroimage*, *40*, 570–582.

Mothersill, O., Kelly, S., Rose, E. J., & Donohoe, G. (2012). The effects of psychosis risk variants on brain connectivity: A review. *Frontiers in Psychiatry*, *3*, 18.

Nelson, M. T., Seal, M. L., Phillips, L. J., Merritt, A. H., Wilson, R., & Pantelis, C. (2011). An investigation of the relationship between cortical connectivity and schizotypy in the general population. *The Journal of Nervous and Mental Disease*, *199*, 348–353.

Nomi, J. S., Vij, S. G., Dajani, D. R., Steimke, R., Damaraju, E., Rachakonda, S., … Uddin, L. Q. (2017). Chronnectomic patterns and neural flexibility underlie executive function. *Neuroimage*, *147*, 861–871.

Patel, A. X., Kundu, P., Rubinov, M., Jones, P. S., Vértes, P. E., Ersche, K. D., … Bullmore, E. T. (2014). A wavelet method for modeling and despiking motion artifacts from resting-state fMRI time series. *Neuroimage*, *95*, 287–304.

Pawlak, V., & Kerr, J. N. (2008). Dopamine receptor activation is required for corticostriatal spike-timing-dependent plasticity. *Journal of Neuroscience*, *28*, 2435–2446.

Pettersson-Yeo, W., Allen, P., Benetti, S., McGuire, P., & Mechelli, A. (2011). Dysconnectivity in schizophrenia: Where are we now? *Neuroscience & Biobehavioral Reviews*, *35*, 1110–1124.

Polner, B., Faiola, E., Urquijo, M. F., Meyhöfer, I., Steffens, M., Rónai, L., … Ettinger, U. (2019). The network structure of schizotypy in the general population. *European Archives of Psychiatry and Clinical Neuroscience*, 1–11.

Power, J. D., Barnes, K. A., Snyder, A. Z., Schlaggar, B. L., & Petersen, S. E. (2012). Spurious but systematic correlations in functional connectivity MRI networks arise from subject motion. *Neuroimage*, *59*, 2142–2154.

Power, J. D., Cohen, A. L., Nelson, S. M., Wig, G. S., Barnes, K. A., Church, J. A., … Petersen, S. E. (2011). Functional network organization of the human brain. *Neuron*, *72*, 665–678.

https://doi.org/10.1017/S0033291720002445 Published online by Cambridge University Press

Raine, A. (1991). The SPQ: A scale for the assessment of schizotypal personality based on DSM-III-R criteria. *Schizophrenia Bulletin*, *17*, 555–564.

Raine, A., Reynolds, C., Lencz, T., Scerbo, A., Triphon, N., & Kim, D. (1994). Cognitive-perceptual, interpersonal, and disorganized features of schizotypal personality. *Schizophrenia Bulletin*, *20*, 191–201.

Rolland, B., Amad, A., Poulet, E., Bordet, R., Vignaud, A., Bation, R., … Jardri, R. (2015). Resting-state functional connectivity of the nucleus accumbens in auditory and visual hallucinations in schizophrenia. *Schizophrenia Bulletin*, *41*, 291–299.

Sarig, S., Dar, R., & Liberman, N. (2012). Obsessive-compulsive tendencies are related to indecisiveness and reliance on feedback in a neutral color judgment task. *Journal of Behavior Therapy and Experimental Psychiatry*, *43*, 692–697.

Seghier, M. L. (2013). The angular gyrus: Multiple functions and multiple subdivisions. *Neuroscientist*, *19*, 43–61.

Shan, H. D., Zhang, R. T., Jiang, S. Y., Wang, Y. M., Liu, Y. F., Cheung, E. F., & Chan, R. C. (2020). Schizotypal and obsessive-compulsive traits: Co-occurrence rate and relationship with executive function, emotion experience and emotion expressivity in college students. *Psych Journal*. doi:10.1002/pchj.372.

Shi, L. J., Liu, W. H., Shi, H. S., Yan, C., Wang, Y., Wang, Y., … Chan, R. C. (2017). Co-occurrence of autistic and schizotypal traits and its association with emotional and psychosocial function in Chinese college students. *Psychiatry Research*, *248*, 64–70.

Smith, S. M., Jenkinson, M., Johansen-Berg, H., Rueckert, D., Nichols, T. E., Mackay, C. E., … Behrens, T. E. J. (2006). Tract-based spatial statistics: Voxelwise analysis of multi-subject diffusion data. *Neuroimage*, *31*, 1487–1505.

Stephan, K. E., Friston, K. J., & Frith, C. D. (2009). Dysconnection in schizophrenia: From abnormal synaptic plasticity to failures of self-monitoring. *Schizophrenia Bulletin*, *35*, 509–527.

Timmler, S., & Simons, M. (2019). Grey matter myelination. *Glia*, *67*, 2063–2070.

Tseng, K. Y., & O'Donnell, P. (2004). Dopamine-glutamate interactions controlling prefrontal cortical pyramidal cell excitability involve multiple signaling mechanisms. *Journal of Neuroscience*, *24*, 5131–5139.

Uddin, L. Q., Nomi, J. S., Hebert-Seropian, B., Ghaziri, J., & Boucher, O. (2017). Structure and function of the human insula. *Journal of Clinical Neurophysiology: Official Publication of the American Electroencephalographic Society*, *34*, 300–306.

Verhoeven, K. J., Simonsen, K. L., & McIntyre, L. M. J. O. (2005). Implementing false discovery rate control: Increasing your power. *Oikos*, *108*, 643–647.

Wang, Y., Ettinger, U., Meindl, T., & Chan, R. C. (2018a). Association of schizotypy with striatocortical functional connectivity and its asymmetry in healthy adults. *Human Brain Mapping*, *39*, 288–299.

Wang, K., Wang, Y., Yan, C., Wang, Y. N., Cheung, E. F., & Chan, R. C. (2013). Semantic processing impairment in individuals with schizotypal personality disorder features: A preliminary event-related potential study. *Progress in Neuro-Psychopharmacology and Biological Psychiatry*, *40*, 93–102.

Wang, Y., Yan, C., Yin, D. Z., Fan, M. X., Cheung, E. F., Pantelis, C., & Chan, R. C. (2014). Neurobiological changes of schizotypy: Evidence from both volume-based morphometric analysis and resting-state functional connectivity. *Schizophrenia Bullentin*, *41*, S444–S454.

Wang, Y. M., Yang, Z. Y., Cai, X. L., Zhou, H. Y., Zhang, R. T., Yang, H. X., … Chan, R. C. (2020a). Identifying schizo-obsessive comorbidity by tract-based spatial statistics and probabilistic tractography. *Schizophrenia Bulletin*, *46*, 442–453.

Wang, Y. M., Zhang, Y. J., Cai, X. L., Yang, H. X., Cheung, E. F., & Chan, R. C. (2020b). Altered grey matter volume and white matter integrity in individuals with high schizo-obsessive traits, high schizotypal traits and obsessive-compulsive symptoms. *Asian Journal of Psychiatry*, *52*, 102096.

Wang, Y. M., Zou, L. Q., Xie, W. L., Yang, Z. Y., Cheung, E. F., Sørensen, T. A., … Chan, R. C. (2018b). Altered functional connectivity of the default mode network in patients with schizo-obsessive comorbidity; A comparison between schizophrenia and obsessive-compulsive disorder. *Schizophrenia Bulletin*, *45*, 199–210.

Wei, J., Lin, C. H., Wu, H., Jin, Y., Lee, Y. H., & Wu, J. Y. (2006). Activity-dependent cleavage of brain glutamic acid decarboxylase 65 by calpain. *Journal of Neurochemistry*, *98*, 1688–1695.

Wolf, M. E. (2003). Effects of psychomotor stimulants on glutamate receptor expression. *Methods in Molecular Medicine*, *79*, 13–31.

Wolf, M. E., Mangiavacchi, S., & Sun, X. (2003). Mechanisms by which dopamine receptors may influence synaptic plasticity. *Annals of the New York Academy of Sciences*, *1003*, 241–249.

Wong, K. K., & Raine, A. (2018). Developmental aspects of schizotypy and suspiciousness: A review. *Current Behavioral Neuroscience Reports*, *5*, 94–101.

Woodward, N. D., Rogers, B., & Heckers, S. (2011). Functional resting-state networks are differentially affected in schizophrenia. *Schizophrenia Research*, *130*, 86–93.

Xia, M., Wang, J., & He, Y. (2013). Brainnet viewer: A network visualization tool for human brain connectomics. *PLoS ONE*, *8*, e68910.

Yan, C. G., Cheung, B., Kelly, C., Colcombe, S., Craddock, R. C., Di Martino, A., … Milham, M. P. (2013). A comprehensive assessment of regional variation in the impact of head micromovements on functional connectomics. *Neuroimage*, *76*, 183–201.

Yan, C. G., & Zang, Y. F. (2010). DPARSF: A MATLAB toolbox for "pipeline" data analysis of resting-state fMRI. *Frontiers in Systems Neuroscience*, *4*, 13.

Yin, Y., Jin, C., Hu, X., Duan, L., Li, Z., Song, M., … Li, L. J. (2011). Altered resting-state functional connectivity of thalamus in earthquake-induced posttraumatic stress disorder: A functional magnetic resonance imaging study. *Brain Research*, *1411*, 98–107.

Zalesky, A., Fornito, A., & Bullmore, E. T. (2010). Network-based statistic: Identifying differences in brain networks. *Neuroimage*, *53*, 1197–1207.

Zhu, Y. K., Tang, Y. X., Zhang, T. H., Li, H., Tang, Y. Y., Li, C. B., … Wang, J. J. (2017). Reduced functional connectivity between bilateral precuneus and contralateral parahippocampus in schizotypal personality disorder. *BMC Psychiatry*, *17*, 48.

https://doi.org/10.1017/S0033291720002445 Published online by Cambridge University Press